 Related Commentary, page 3585

MicroRNA15a modulates expression of the cell-cycle regulator Cdc25A and affects hepatic cystogenesis in a rat model of polycystic kidney disease

Seung-Ok Lee,[1,2] Tatyana Masyuk,[1] Patrick Splinter,[1] Jesús M. Banales,[1,3] Anatoliy Masyuk,[1] Angela Stroope,[1] and Nicholas LaRusso[1]

[1]Miles and Shirley Fiterman Center for Digestive Diseases, Division of Gastroenterology and Hepatology, Mayo Clinic College of Medicine, Rochester, Minnesota, USA. [2]Chonbuk National University Medical School, Jeonju, Jeonbuk, Republic of Korea. [3]Laboratory of Molecular Genetics, Division of Gene Therapy and Hepatology, University of Navarra School of Medicine, Clínica Universitaria and CIMA, Centro de Investigación Biomédica en Red, Pamplona, Spain.

Hyperproliferation of bile duct epithelial cells due to cell-cycle dysregulation is a key feature of cystogenesis in polycystic liver diseases (PCLDs). Recent evidence suggests a regulatory role for microRNAs (miRNAs) in a variety of biological processes, including cell proliferation. We therefore hypothesized that miRNAs may be involved in the regulation of selected components of the cell cycle and might contribute to hepatic cystogenesis. We found that the cholangiocyte cell line PCK-CCL, which is derived from the PCK rat, a model of autosomal recessive polycystic kidney disease (ARPKD), displayed global changes in miRNA expression compared with normal rat cholangiocytes (NRCs). More specific analysis revealed decreased levels of 1 miRNA, miR15a, both in PCK-CCL cells and in liver tissue from PCK rats and patients with a PCLD. The decrease in miR15a expression was associated with upregulation of its target, the cell-cycle regulator cell division cycle 25A (Cdc25A). Overexpression of miR15a in PCK-CCL cells decreased Cdc25A levels, inhibited cell proliferation, and reduced cyst growth. In contrast, suppression of miR15a in NRCs accelerated cell proliferation, increased Cdc25A expression, and promoted cyst growth. Taken together, these results suggest that suppression of miR15a contributes to hepatic cystogenesis through dysregulation of Cdc25A.

Introduction

Polycystic liver diseases (PCLDs) are genetically heterogeneous and occur alone or in combination with polycystic kidney disease (PKD) (1, 2). Autosomal dominant PCLD (ADPLD) displays no renal involvement and is caused by a mutation of the gene protein kinase substrate 80K-H (*PRKCSH*), which encodes the protein hepatocystin (3). PKD is a genetic nephrohepatic cystic disease and can be inherited in an autosomal dominant (ADPKD) or autosomal recessive (ARPKD) fashion. ADPKD is more common and is linked to mutations in either *PKD1* or *PKD2*, genes that encode the proteins polycystin 1 and polycystin 2, respectively (4). ARPKD is caused by mutations of the gene polycystic kidney and hepatic disease 1 (*PKHD1*), which encodes the protein fibrocystin/polyductin (5, 6). ARPKD has a high mortality rate, with approximately 30% of affected neonates dying within hours after birth because of respiratory difficulties due to enlarged kidneys. In surviving patients, hepatic lesions become progressively more severe with age; liver disease is the major cause of morbidity and mortality and is characterized by biliary dysgenesis associated with congenital hepatic fibrosis (CHF), bile duct dilatation, and cyst formation (2, 7).

The mechanisms involved in the pathogenesis of liver cysts in the PCLDs are unclear. However, it is likely that hyperproliferation of bile duct epithelial cells (i.e., cholangiocytes) plays a major role in hepatic cyst growth and expansion. Indeed, in the PCK rat, a well-characterized animal model of ARPKD (6, 8), bile ducts are markedly distorted, displaying multiple saccular dilatations and many hepatic cysts of different sizes (9). Moreover, overgrowth of liver cysts is associated with increased proliferative activity of cystic cholangiocytes in PCK rats compared with age-matched normal rats (10, 11). Finally, in a spontaneously immortalized cholangiocyte cell line derived from the PCK rat (PCK-CCL) that retains the in vivo phenotype of cystic cholangiocytes, the rate of cell proliferation is significantly higher and the doubling time twice as fast as in a cell line derived from normal rats (normal rat cholangiocytes [NRCs]) (12).

It is known that accelerated cell proliferation is related to alterations in the cell cycle. Cell proliferation is a complex process that is regulated by different cellular components, including protein kinases and phosphatases. Cell division cycle 25 (Cdc25), a family of dual-specificity phosphatases, plays an essential role in cell-cycle progression by activating cyclin-dependent kinases (Cdks) (13). Three Cdc25 isoforms (Cdc25A, Cdc25B, and Cdc25C) have been identified (14, 15). Although Cdc25B and Cdc25C contribute to cell-cycle regulation, Cdc25A is principally responsible for G1-S and G2-M transitions (16). Importantly, the overexpression of Cdc25A and Cdc25B in a number of cancers is frequently correlated with tumor grade and aggressiveness as well as with poor prognosis (17). Thus, Cdc25 phosphatases have become a new

Nonstandard abbreviations used: ADPKD, autosomal dominant PKD; ARPKD, autosomal recessive PKD; Cdc25A, cell division cycle 25A; Cdk, cyclin-dependent kinase; CHF, congenital hepatic fibrosis; EV, empty vector; miRNA, microRNA; NRC, normal rat cholangiocyte; PCLD, polycystic liver disease; PKD, polycystic kidney disease.

Conflict of interest: The authors have declared that no conflict of interest exists.

Citation for this article: *J. Clin. Invest.* **118**:3714–3724 (2008). doi:10.1172/JCI34922.

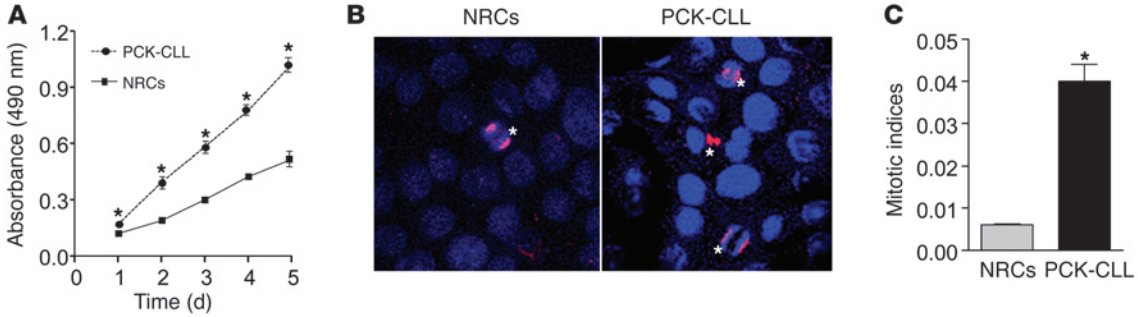

Figure 1
Rates of cell proliferation and mitotic indices in NRCs and PCK-CCL. (**A**) In PCK-CCL, the rate of cell proliferation (determined by MTS absorbance at 490 nm) was significantly higher at each time point. Data are representative of 5 independent experiments. (**B**) Mitotic figures (asterisks) in NRCs and PCK-CCL were assessed by immunofluorescent confocal microscopy using an anti–α-tubulin antibody as a marker for microtubules (red). Nuclei were stained with DAPI (blue). Original magnification, ×60. (**C**) Quantitative analysis shows that in PCK-CCL, the number of mitotic cells (>500 cells counted in each experiment) was significantly greater compared with NRCs. *$P < 0.05$.

pharmacological target in cancer therapy (18). However, there are no data on the Cdc25 activity associated with benign, hyperproliferative diseases such as the PCLDs.

Accumulating evidence suggests that expression of genes involved in many cellular processes is regulated by small noncoding RNAs (i.e., microRNAs [miRNAs]) that posttranscriptionally inhibit target mRNA transcripts via sequence-specific base pairing (19). Biochemical and genetic studies suggest that miRNAs play important roles in a variety of cellular processes, including differentiation, apoptosis, and cell proliferation (20). In particular, the miR17 cluster and miR21 are known to promote cell proliferation (21), while miR15a, miR16, and the family of let-7 miRNAs suppress cell proliferation (22, 23). Moreover, many cancers are characterized by aberrant expression of miRNAs, with a majority of the miRNAs being substantially reduced (24, 25). However, no data describing the profiling and role of miRNAs in the pathogenesis of PCLDs exist.

In the present study, we employed in vivo (the PCK and normal rats) and in vitro (cholangiocyte cell lines derived from PCK [PCK-CCL] and from normal [NRCs] rats) models to examine the following: (a) miRNA profiles; (b) expression of Cdc25A message and protein; (c) role of miR15a in posttranscriptional regulation of Cdc25A; (d) effect of experimental modulation of miR15a levels on cell-cycle distribution and rate of cholangiocyte proliferation; and (e) effect of miR15a modulation on cyst growth and expansion. We also assessed expression of miR15a and Cdc25A in normal human livers and in livers of patients with ADPKD, ARPKD, and CHF.

Our data show a relationship between cholangiocyte proliferation and upregulation of Cdc25A, an important cell-cycle regulator. Moreover, these data suggest that Cdc25A overexpression is due to posttranscriptional inhibition by miR15a and that this regulatory pathway is involved in hepatic cystogenesis.

Results

The rate of cell proliferation and the mitotic index are increased in PCK-CCL. Rates of cell proliferation in PCK-CCL and NRCs were measured over time. Consistent with our previous observation (12), PCK-CCL showed higher proliferation rates (~2-fold) at every time point analyzed (Figure 1A). The calculated doubling time was twice as fast in PCK-CCL (~28.8 hours) compared with that of NRCs (~58.1 hours; $P < 0.05$).

To evaluate mitotic rates in PCK-CCL, the number of cells with mitotic spindles (i.e., mitotic indices) was assessed by immunofluorescent confocal microscopy. Our data demonstrated that in PCK-CCL, mitotic indices were approximately 5-fold greater compared with in NRCs (Figure 1, B and C).

Expression of miRNAs is altered in PCK-CCL. To identify potential miRNAs that might regulate the expression of proteins involved in cell-cycle progression and thus influence the accelerated rate of proliferation in PCK-CCL, we performed microarray analysis of miRNA profiles in NRCs and PCK-CCL and found that the expression of miRNAs in PCK-CCL was markedly different from that in NRCs (Supplemental Table 1; supplemental material available online with this article; doi:10.1172/JCI34922DS1). In total, subsets of 121 and 148 miRNAs were detected in NRCs and PCK-CCL, respectively. Twelve miRNAs were present in NRCs but not in PCK-CCL, and 39 miRNAs were present only in PCK-CCL. Moreover, 109 miRNAs common to both cell lines were differentially expressed in PCK-CCL. Interestingly, of the differentially expressed miRNAs, most (i.e., 97 miRNAs, or 89%) were downregulated in PCK-CCL compared with NRCs, and 12 miRNAs (11%) were overexpressed in cystic cholangiocytes.

Expression of miRNA15a is reduced in vitro and in vivo in cystic cholangiocytes. Microarray analysis revealed that the level of 1 of the miRNAs present in both cell lines, miR15a, was decreased 37-fold in PCK-CCL compared with in NRCs, being by far the most suppressed miRNA (Figure 2, A and B). To validate the microarray platform, we assessed the expression of miR15a in NRCs and PCK-CCL by Northern blot analysis. By this approach, we confirmed a decrease in miR15a expression in PCK-CCL, although the difference was smaller (~4-fold; Figure 2C). We also examined levels of miR15a in freshly isolated cholangiocytes of normal and PCK rats by quantitative PCR. Consistent with our in vitro data, expression of miR15a in cystic cholangiocytes of PCK rats was decreased approximately 8-fold compared with in normal rats (Figure 2D). Thus, reduced expression of miR15a in cystic cholangiocytes was observed by several independent techniques in vitro and in vivo.

To assess the levels of miR15a in whole-liver tissue of normal and PCK rats and in liver tissue of normal humans and patients with ADPKD, ARPKD, and CHF, we applied locked nucleic acid in situ hybridization (LNA-ISH). Locked nucleic acid–modified oligonucleotide probes have been successfully used to visualize

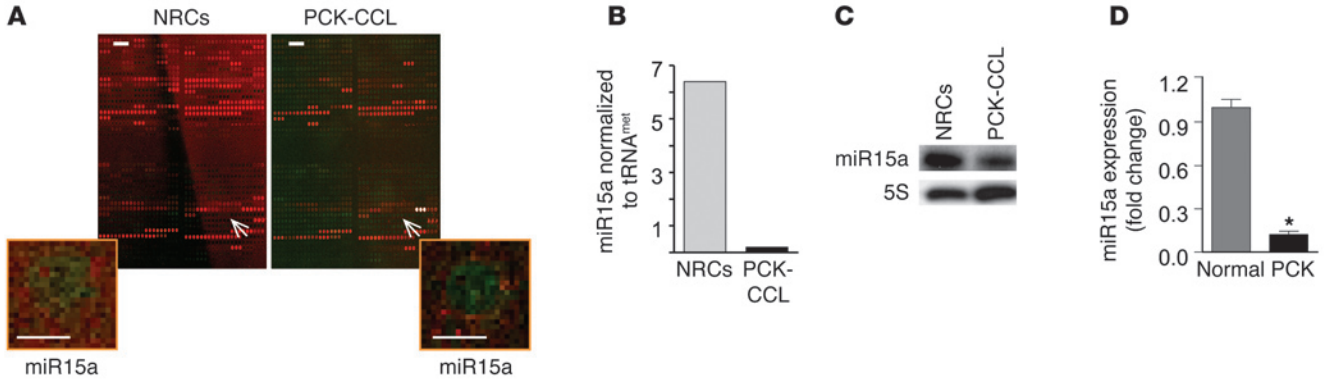

Figure 2
Expression of miR15a in normal and cystic cholangiocytes in vitro and in vivo. (**A** and **B**) As shown by microarray analysis, miR15a was down-regulated 37-fold in PCK-CCL compared with NRCs. Scale bars: 1000 μm (microarray images); 100 μm (insets). (**C**) Using Northern blot, we detected smaller (~4-fold) changes in expression of miR15a in PCK-CCL. (**D**) Consistent with in vitro data, miR15a levels were decreased in cholangiocytes freshly isolated from PCK rats compared with those in normal rats as assessed by quantitative PCR. *$P < 0.05$.

miRNAs in whole-mount preparations of zebrafish (26) and in human brain tissue (27). Unlike with the mismatch control probe (i.e., scrambled miRNA), hybridization with the miR15a-specific probe revealed the presence of miR15a in normal and cystic cholangiocytes. However, the intensity of miR15a immunoreactivity in cholangiocytes lining liver cysts in patients with ADPKD, ARPKD, and CHF and in the PCK rat was reduced compared with that in normal human cholangiocytes and NRCs (Figure 3).

Cdc25A is one of the potential targets of miR15a. By an in silico approach, we identified that 1 of the potential targets of miR15a is the family of Cdc25 dual-specificity phosphatases that play an essential role in cell-cycle progression. Moreover, miR15a has a conserved complementarity to Cdc25A mRNA (Table 1). Using a rat genomic DNA database search, the 83-bp miR15a precursor sequence, including 22-bp miR15a, was detected at rat chromosome 15. Sequencing of the miR15a precursor region showed no polymorphisms in the genomic DNA from NRCs and PCK-CCL.

We also searched for any other miRNAs that could potentially bind to Cdc25A mRNA. Thirty-one miRNAs with partial or complete complementarity to Cdc25A mRNA were found. However, only 8 of them were present in both cell lines (Table 2). Two of them, miR34a and miR107, were expressed only in PCK-CCL.

Cdc25A protein expression is increased in cystic cholangiocytes in vitro and in vivo, while Cdc25A mRNA levels are not different. Next, we analyzed the expression of Cdc25A at the message and protein levels in NRCs and PCK-CCL and in freshly isolated cholangiocytes from normal and PCK rats. By RT-PCR, we found no significant differences in Cdc25A mRNA levels between NRCs and PCK-CCL (Figure 4, A and B). This result was confirmed in freshly isolated cholangiocytes (Figure 4, C and D). However, the expression of Cdc25A protein assessed by Western blot was significantly higher in PCK-CCL (~3 times) and PCK cholangiocytes (~2 times) compared with NRCs and cholangiocytes isolated from normal rats, respectively (Figure 4, E–H). The differences in Cdc25A expression at mRNA and protein levels suggested that miRNAs might be involved in posttran-

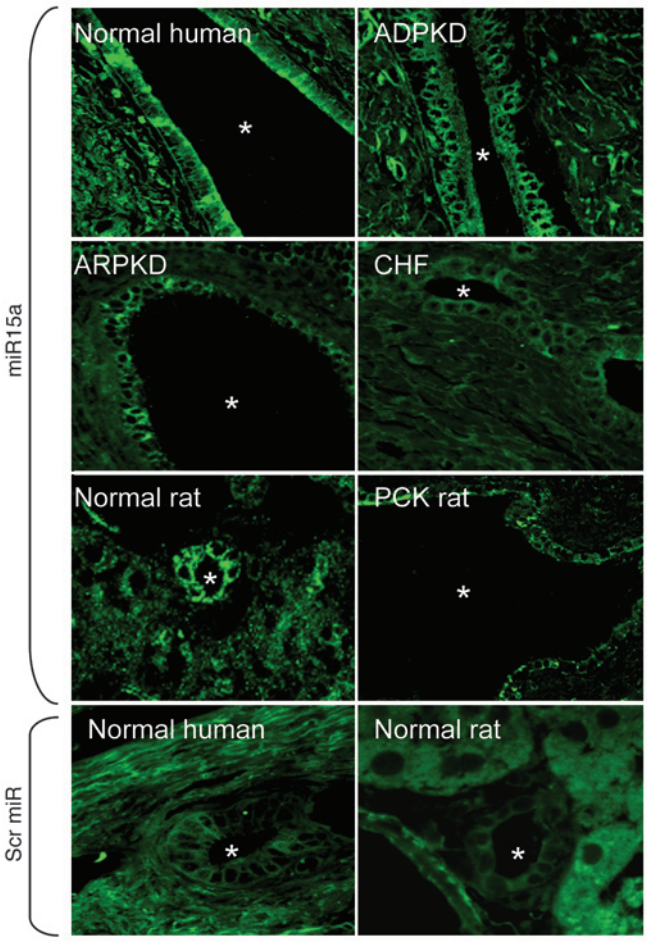

Figure 3
Expression of miR15a in human and rat liver tissue by locked nucleic acid in situ hybridization. Intensity of miR15a immunoreactivity in cholangiocytes lining liver cysts in patients with ADPKD, ARPKD, and CHF and in the PCK rat was reduced compared with that in normal human cholangiocytes and NRCs. No staining was observed in liver tissue hybridized with scrambled (scr) miRNA. Original magnification, ×100 (normal human and normal rat); ×63 (ADPKD, ARPKD, CHF, and PCK rat). Asterisks indicate bile duct or cyst lumen. Data are representative of 3 independent experiments.

Table 1
miR15a:Cdc25A-mRNA complementarity in human and rat

mRNA		Sequence
miR15a		GUGUUUGGUAA**UA****CACGACGA**U 5′
Rno Cdc25A	5′	**C**AC**UGAAGUGCUGCU**G
Mmu Cdc25A	5′	CGCCC**AAGUGCUGCU**G
Hsa Cdc25A	5	GAAGUUACACAG**A**AA**UGCUGCU**G

Seed match is denoted by bold letters.

scriptional regulation of the Cdc25A protein. Expression of Cdc25A was also assessed by immunofluorescent confocal microscopy in liver tissue of the PCK and normal rats and in liver tissue of normal humans and patients with ARPKD, ADPKD, and CHF. Representative images in Figure 5 show that immunoreactivity of Cdc25A was higher in cholangiocytes lining liver cysts in humans and PCK rats compared with normal human cholangiocytes and NRCs.

Modulation of miR15a alters the expression of Cdc25A protein in transiently transfected PCK-CCL. To support the notion that posttranscriptional regulation of Cdc25A by miR15a might contribute to increased Cdc25A protein expression, PCK-CCL was transfected with FITC-labeled miR15a, and Cdc25A expression was assessed by confocal immunofluorescent microscopy. As shown in Figure 6, A and B, we observed significantly reduced fluorescent immunoreactivity of Cdc25A in FITC-labeled miR15a-transfected cells compared with nontransfected PCK-CCL.

To further support the notion that miR15a posttranscriptionally regulates the level of Cdc25A protein, we transfected PCK-CCL with a miR15a precursor (pre-miR15a) and assessed the levels of miR15a by quantitative PCR. PCK-CCL transfected with scrambled miRNA was used as a control. Data presented in Figure 6C demonstrate that levels of miR15a were increased in pre-miR15a PCK-CCL compared with cystic cholangiocytes transfected with scrambled miRNA. Consistent with our prediction, overexpression of miR15a in PCK-CCL was associated with an approximately 50% reduction in the level of Cdc25A protein (Figure 6, D and E).

Modulation of miR15a alters the cell cycle in transiently transfected PCK-CCL. Cdc25A is an important cell-cycle regulator and plays a major role in G1-S transition. Based on our data that experimental modulation of miR15a altered Cdc25A protein expression, we predicted that it would also affect the cell cycle in PCK-CCL. To this end, we assessed the cell-cycle phase distribution in pre-miR15a PCK-CCL by FACS analysis and found that the portion of G1 phase cells was increased by 23% while the portion of cells in S phase was reduced by 37.2% compared with that in PCK-CCL treated with scrambled miRNA only (Figure 6F). These data suggest that suppression of Cdc25A by miR15a induces inhibition of G1-S cell-cycle transition, resulting in accumulation of cholangiocytes in the G1 phase.

miR15a suppresses Cdc25A by binding to the 3′-UTR region. To directly address whether miR15a binds to the Cdc25A mRNA, leading to its translational suppression, we generated a pMIR-REPORT luciferase construct containing Cdc25A mRNA 3′-UTR region with the putative miR15a-binding site (Cdc25A WT). In addition, we generated another pMIR-REPORT luciferase construct containing Cdc25A mRNA 3′-UTR region with a mutation at the putative miR15a-binding site (Cdc25A mutant; Figure 7A). As shown in Figure 7B, in PCK-CCL cotransfected with miR15a precursor and Cdc25A WT construct, luciferase reporter translation was decreased by 75.1% compared with that in PCK-CCL transfected with Cdc25A WT construct only. However, in PCK-CCL cotransfected with miR15a precursor and Cdc25A mutant construct, expression of luciferase reporter was not inhibited. We also did not observe any significant changes in expression of luciferase reporter in PCK-CCL cotransfected with scrambled miRNA and Cdc25A WT or Cdc25A mutant. These data suggest that miR15a regulates Cdc25A protein expression through direct binding to the 3′-UTR region of Cdc25A mRNA.

Cell proliferation is decreased in stably transfected PCK-CCL overexpressing miR15a. To evaluate the effect of miR15a on cell proliferation and cyst growth, we established a stable cell line (PCK-CCL–pSR-miR15a) that overexpressed miR15a. Quantitative PCR demonstrated that expression of miR15a was increased in PCK-CCL–pSR-miR15a compared with nontransfected PCK-CCL or PCK-CCL transfected with empty vector (EV) (PCK-CCL–pSR-EV; Figure 8A). Importantly, in PCK-CCL–pSR-miR15a, the rate of cholangiocyte proliferation was inhibited compared with that in PCK-CCL–pSR-EV (Figure 8B) and the doubling time was increased from 25 hours to 31 hours ($P < 0.05$).

The rate of cyst growth is decreased in PCK-CCL overexpressing miR15a. We have previously shown that PCK-CCL seeded in 3D culture organizes into cystic structures that continue to expand progressively over time (12). Thus, we evaluated the effect of miR15a overexpression on growth of cysts formed by both PCK-CCL–pSR-miR15a and PCK-CCL–pSR-EV. Cystic surface area was assessed at days 3, 6, 9 and 12 for each cell line. We found that 75% of cysts formed by PCK-CCL–pSR-EV progressively grew over time (Figure 8C). In contrast, all cysts formed by PCK-CCL–pSR-miR15a did not expand, as assessed by light microscopy and quantitative analysis of cystic surface areas (Figure 8D). Importantly, inhibition of cyst growth was more dramatic than the effect of miR15a on the rate of cholangiocyte proliferation, suggesting that miR15a may affect expression of other genes related to cystogenesis.

Cell proliferation, Cdc25A protein expression, and cyst growth are affected by downregulation of miR15a in NRCs. To further prove that miR15a is involved in regulation of Cdc25A protein expression and subsequently affects cell proliferation and cyst growth, we reduced miR15a levels in normal cholangiocytes with a miR15A antisense (anti-miR15a). Figure 9A demonstrates that both anti-miR15a and scrambled miRNA labeled with Cy3 dye were present in treated cholangiocytes compared with nontreated cells.

Table 2
Expression profile of miRNAs that can potentially bind Cdc25A mRNA

miRNAs	Ratio[A]		Fold change
	NRCs	PCK-CCL	
miR15a	6.4	0.2	–37.3
miR34a	–	0.2	
miR103	0.5	0.4	–1.1
miR107	–	1.0	
miR195	0.4	0.1	–3.3
miR204	59.0	6.5	–9.0
miR326	47.3	5.9	–8.0
miR331	1.2	0.4	–3.2

[A]Ratio represents gene signal intensity normalized to $tRNA^{met}$ signal intensity.

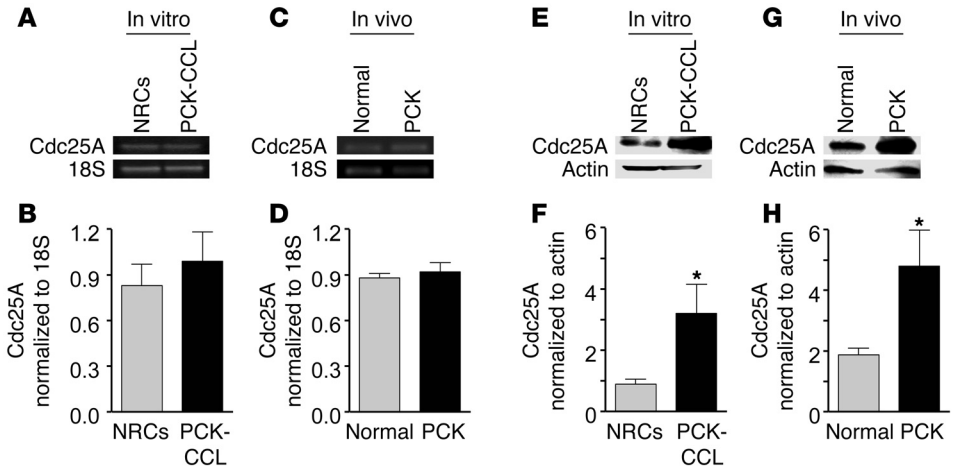

Figure 4
Expression levels of Cdc25A message and protein in vitro (NRCs and PCK-CCL) and in vivo (freshly isolated cholangiocytes from normal and PCK rats). Using RT-PCR, we found no significant differences in Cdc25A mRNA levels in the PCK–CCL (**A** and **B**) and PCK rats (**C** and **D**) compared with NRCs and normal rats, respectively. In contrast, levels of Cdc25A protein expression were significantly higher in the PCK–CCL (**E** and **F**) and PCK rats (**G** and **H**) compared with NRCs and normal rats, respectively. Data are representative of 3 independent experiments. $^*P < 0.05$.

Quantitative PCR revealed that miR15a expression was decreased in NRCs exposed to anti-miR15a compared with cholangiocytes exposed to vehicle or scrambled miRNA (Figure 9B). Downregulation of miR15a in normal cholangiocytes affected Cdc25A protein expression, cholangiocyte proliferation, and cyst growth. As shown in Figure 9, C and D, in the presence of anti-miR15a, the level of its target, Cdc25A, was significantly increased compared with levels in scrambled miRNA. Upregulation of Cdc25A was accompanied by a mildly increased rate of cholangiocyte proliferation (Figure 9E). We also examined the effect of miR15a inhibition on cyst growth by assessing the changes in the area of cystic structures formed by normal cholangiocytes in 3D culture during 5 days (days 0–4). In the presence of both scrambled miRNA and anti-miR15a, normal cholangiocytes progressively expanded over time. However, the rate of cyst growth was significantly accelerated in cholangiocytes treated with anti-miR15a (Figure 9, F and G). These data further support the notion that the miR15a/Cdc25A complex plays an important role in regulation of cholangiocyte proliferation and cyst growth.

Discussion

In the present study, we found the following: (a) cholangiocytes derived from the PCK rat display global changes in miRNA expression compared with NRCs; (b) miR15a has complementarity to Cdc25A mRNA and is downregulated in vitro in PCK-CCL and in vivo in bile ducts of the PCK rat; (c) increased cholangiocyte proliferation is accompanied by overexpression of Cdc25A in PCK-CCL; (d) reduced miR15a expression is associated with increased levels of Cdc25A in patients with ADPKD, ARPKD, and CHF; (e) experimental modulation of miR15a changes the levels of Cdc25A protein; (f) overexpression of miR15a in cystic cholangiocytes inhibits G1-S cell-cycle transition, cholangiocyte proliferation, and cyst growth; and (g) downregulation of miR15a in normal cholangiocytes increases cell proliferation and Cdc25A expression and accelerates cyst growth. Overall, our data suggest that the miR15a/Cdc25A complex plays an important role in dysregulation of the cell cycle and subsequent growth of liver cysts in the PCLDs.

Hyperproliferation of cholangiocytes is considered to be one of the major causative mechanisms involved in hepatic cystogenesis in the PCLDs (1). It is also known that increased rates of cell proliferation are related to cell-cycle dysregulation. In the work described here, we demonstrate for what we believe is the first time that Cdc25A, a cell-cycle regulator, is overexpressed in cholangio-

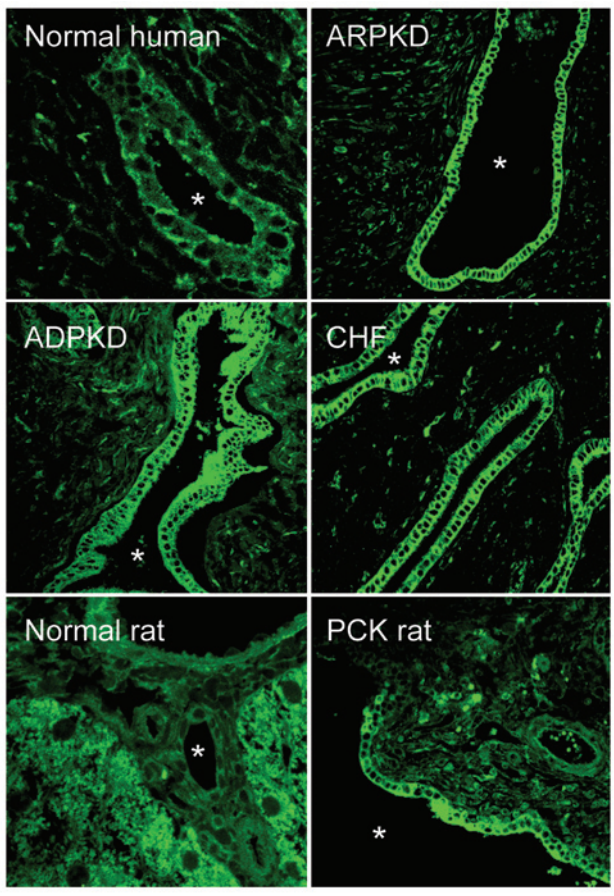

Figure 5
Expression of Cdc25A in liver tissue by immunofluorescent confocal microscopy. Levels of Cdc25A were increased in cholangiocytes lining rat and human liver cysts compared with normal cholangiocytes. Original magnification, ×100 (normal human and normal rat); ×63 (ADPKD, ARPKD, CHF, PCK rat). Asterisks indicate bile duct or cyst lumen. Data are representative of 3 independent experiments.

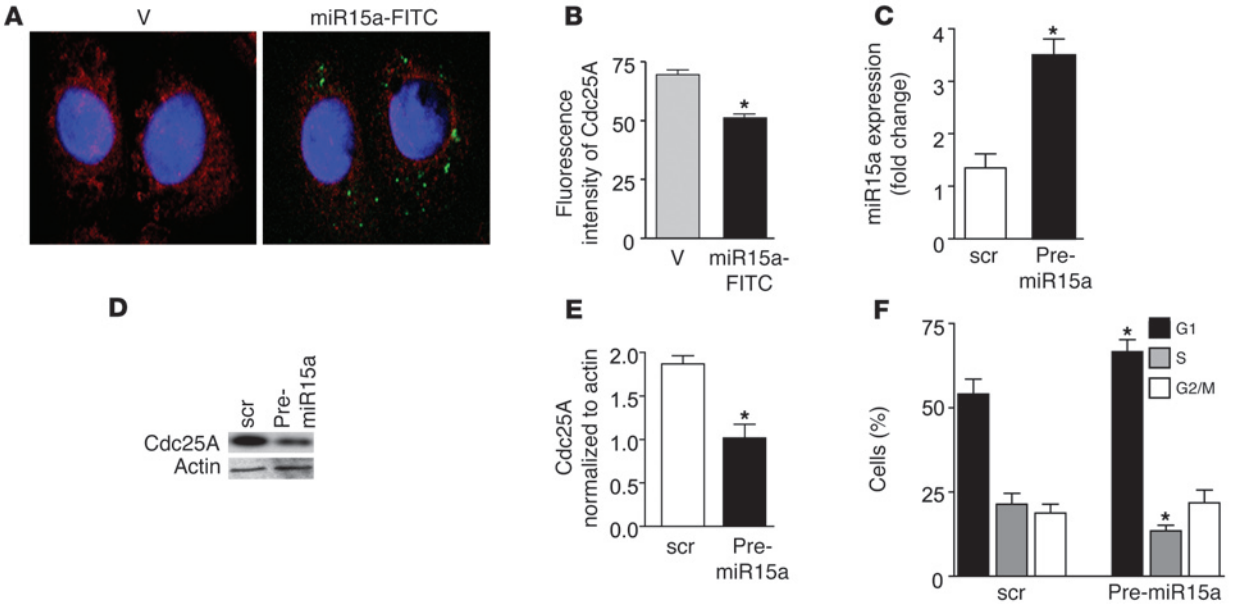

Figure 6

Effect of miR15a modulation on Cdc25A protein expression in transiently transfected PCK-CCL. (**A**) Fluorescence confocal images and quantitative analysis based on fluorescence intensity (**B**) demonstrate that in PCK-CCL transfected with FITC- labeled miR15a (green spots), expression of Cdc25A (red) was significantly decreased (n = 100 cells for each cell line) compared with that in PCK-CCL treated with vehicle (V) only. Original magnification, ×100. (**C**) Using quantitative PCR, we found that levels of miR15a were increased in PCK-CCL transfected with miR15a precursor (pre-miR15a) compared with those in cholangiocytes transfected with scrambled miRNA. Data are representative of 3 independent experiments. (**D**) Representative Western blot and quantitative analysis (**E**) based on densitometry measurements of 3 independent experiments demonstrate that protein levels of Cdc25A in the pre-miR15a PCK-CCL were decreased by 50%. (**F**) In the pre-miR15a PCK-CCL, the portion of G1 phase cells was increased while the portion of S phase cells was reduced compared with those in PCK-CCL treated with scrambled miRNA. Data are representative of 5 independent experiments. *P < 0.05.

cytes lining liver cysts in the PCK rat and in patients with cystic liver diseases. Moreover, we identified a potential mechanism of Cdc25A upregulation, namely, posttranscriptional regulation of its expression by miR15a. Indeed, experimental inhibition of miR15a in normal cholangiocytes increases Cdc25A protein levels, subsequently resulting in accelerated cell proliferation and more rapid cyst growth. Further, as a result of Cdc25A suppression by miR15a in PCK-CCL due to its experimental overexpression, we observed inhibition in G1-S transition, cholangiocyte proliferation, and rate of cyst formation. The data raise the possibility of a new therapeutic approach to the nephrohepatic cystic diseases — cell-cycle modulation via miRNAs.

Multiple lines of evidence have demonstrated an important role of miRNAs in the regulation of expression of genes involved in different cellular processes, in particular, in cell proliferation (22, 23, 28). To this end, we examined miRNA profiles in normal and PCK cholangiocytes by microarray analysis and found that the levels of miRNAs in PCK-CCL are remarkably different from that in NRCs. Moreover, 1 of the miRNAs, miR15a (known to be associated with regulation of cell proliferation; ref. 22) was decreased 37-fold in PCK-CCL. Microarray analysis in some cases shows larger changes in gene expression compared with other techniques used to validate gene expression, since fluorescence intensities of microarray probes might be affected by other factors, such as variations in probe concentrations and the efficiency of printing pins (29, 30). Indeed, by Northern blot, we detected smaller changes in expression of miR15a. Importantly, these changes were comparable with changes in levels of miR15a detected in freshly isolated PCK cholangiocytes by quantitative PCR. Downregulation of miR15a in cystic cholangiocytes in vivo was further confirmed by in situ hybridization.

Using an in silico approach, we found that miR15a has complementarity to Cdc25A. To directly address whether miR15a binds to Cdc25A mRNA, resulting in translational suppression, we used a pMIR-REPORT luciferase construct containing the Cdc25A mRNA 3′-UTR region with the putative miR15a-binding site. Our data showed that miR15a directly binds to the 3′-UTR region of Cdc25A mRNA, resulting in specific translational suppression. We recognize that other miRNAs may also be involved in regulation of Cdc25A expression. Indeed, in NRCs and PCK-CCL, 5 other miRNAs that could potentially bind to Cdc25A (miR103, miR195, miR204, miR326, and miR331) were found and were also downregulated in PCK-CCL. The data raise the possibility of posttranscriptional regulation of Cdc25A by multiple miRNAs. Interestingly, *let-7* miRNA was recently implicated in regulation of Cdc25A expression in human lung cancer cells (28).

To further evaluate a potential role of miR15a/Cdc25A complex in liver cystogenesis, we employed a 3D culture system. Consistent with our previous data (12), cystic and normal cholangiocytes grown between 2 layers of collagen/Matrigel formed spherical cystic structures that progressively expanded over time. Inhibition of miR15a in normal cholangiocytes resulted in accelerated cyst growth. In contrast, and consistent with our hypothesis, experimental restoration of miR15a levels in PCK-CCL suppressed cyst growth. These results suggest that the miR15a/Cdc25A complex is involved in hepatic cystogenesis.

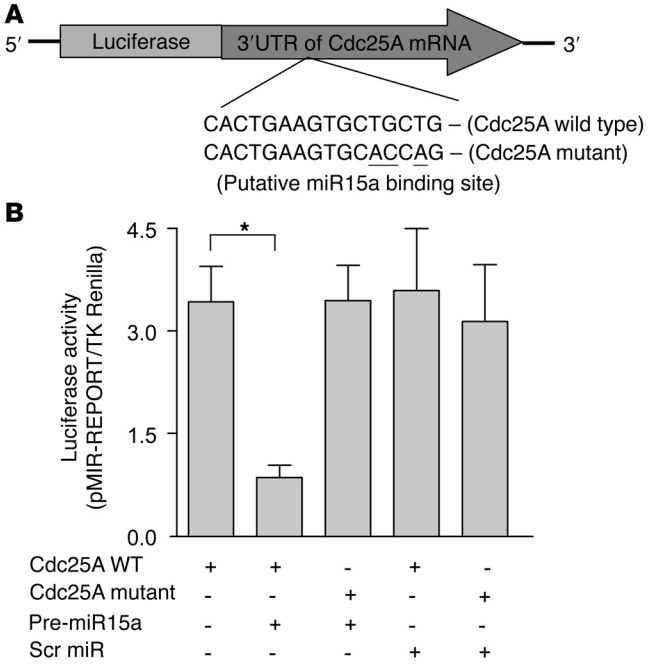

Figure 7
Targeting of miR15a to the 3′-UTR region of Cdc25A mRNA. (**A**) 2 reporter constructs (Cdc25A WT and Cdc25A mutant) with the potential binding site for miR15a in the 3′-UTR region of Cdc25A were generated. (**B**) In PCK-CCL cotransfected with the Cdc25A WT construct and miR15a precursor (pre-miR15a), luciferase reporter translation was significantly decreased compared with that in PCK-CCL transfected with the Cdc25A WT construct only. A mutation in the miR15a–binding sequence in the Cdc25A mRNA 3′-UTR eliminated this effect. Moreover, in the presence of scrambled miRNA (scr miR), no changes in luciferase reporter were observed. Data are representative of 7 independent experiments. *$P < 0.05$.

Our data show that miRNAs are differentially expressed in cystic cholangiocytes, i.e., the majority of miRNAs (89%) are downregulated in PCK-CCL, while 11% of miRNAs are upregulated. Differential expression of miRNAs has also been observed in cancers, with downregulation being more common than upregulation (25, 31, 32). While the precise mechanisms by which miRNAs are altered in cholangiocytes lining liver cysts remain unclear, substantial evidence exists (1, 2, 7, 33, 34) that many cellular processes are disturbed in cystic cells as a result of genetic mutations associated with PCLDs. Thus, it seems reasonable to assume, and our data suggest, that miRNA biogenesis may be one of these cellular processes. miRNAs are transcribed as long primary precursor transcripts (pri-miRNAs) that are cleaved into pre-miRNAs (~70-nt precursor hairpins) by the RNase III–like enzyme Drosha (35). The pre-miRNAs are exported to the cytoplasm by exportin 5 (36) and cleaved to short, partially double-stranded RNA, about 22 nucleotides long, in which 1 strand is the mature miRNA. The mature miRNA then binds to specific messenger RNA targets and mediates either translation repression or direct mRNA cleavage. In principle, since miRNA biogenesis is a highly regulated multistep process, levels of miRNA expression can be regulated at several different levels: (a) pri-miRNA transcription; (b) Drosha-dependent pri-miRNA processing; (c) nuclear export; (d) Dicer-dependent processing into mature miRNAs; and (e) miRNA turnover. Thus, defects at any level of miRNA processing could be responsible for the final levels of miRNA expression. Consistent with this notion, the lack of correlation between pre-miRNA and mature miRNA expression levels was recently observed in human cancer (37). Our results show that in PCK-CCL transfected with pre-miR15a, levels of Cdc25A protein expression (Figure 6), G1-S cell-cycle transition (Figure 6), and cholangiocyte proliferation (Figure 8B) are all decreased. These data suggest that at least at this level (i.e., processing of premature miRNA to mature miRNA), miR15a biogenesis is not affected. However, dysregulation of any other steps of miRNA processing could account for observed changes.

In conclusion, our data suggest that abnormalities in the miR15a/Cdc25A complex play an essential role in the regulation of cell-cycle progression via posttranscriptional modulations of Cdc25A protein expression and thereby contribute to cholangiocyte hyperproliferation and subsequent hepatic cyst growth and expansion. Thus, pharmacologic suppression of cell-cycle progression appears to be a potential therapeutic approach to limiting exaggerated cell proliferation in benign hyperproliferative conditions. Given the key role played by Cdks in the control of the cell-cycle machinery, both Cdks and their regulators, Cdc phosphatases, may represent major pharmacological or biological targets (18). Indeed, effective arrest of renal cystic disease by treatment with a Cdk inhibitor, roscovitine, has recently been reported in *jck* and *cpk* mouse models of PKD (38). However, the effect of roscovitine of hepatic cyst growth was not evaluated in that study. Moreover, to our knowledge, no studies describing the effect of suppression of any of the cell-cycle regulators on progression of liver cysts have been performed. While no miRNA therapies of any pathological conditions have been reported, our data suggest that the modulation of miRNA expression should be considered a potential therapeutic approach in the benign hyperproliferative diseases. Furthermore, since accumulating evidence suggests that miRNA profiling is more specific than mRNA profiling and is very informative, miRNA expression profiling may also be considered as a new diagnostic tool in the PCLDs. Indeed, individual miRNAs and miRNA signatures have already been shown to have prognostic value in some cancers (24, 31).

Methods

Animals and cell culture. WT Sprague-Dawley and PCK rats were maintained on a standard laboratory diet after protocols were approved by the Mayo Institutional Animal Care and Use Committee. Animals were anesthetized with pentobarbital (50 mg/kg BW, intraperitoneally). Normal and cystic cholangiocytes were isolated as previously described (39). Cholangiocyte cell lines derived from the normal rat (NRCs) and the PCK rat (PCK-CCL) were grown as previously described (12). Cultured cells retained the characteristics of cholangiocytes, since they are positive for the epithelial cell marker CK-19 and respond to cAMP activation by accelerating rates of proliferation (data not shown).

Cell proliferation. PCK-CCL and NRCs (2,500 cells/well) were incubated (37°C, 5% CO_2, and 100% humidity) for 48–72 hours before assays. Rates of cell proliferation were determined using CellTiter 96 AQ_{ueous} One Solution Cell Proliferation Assay (Promega), as previously described (12). To study the effect of miR15a suppression in normal cholangiocytes, NRCs were treated with 50 nM of either anti-miR15a (Ambion; Applied Biosystems) or scrambled miRNA at day 0 and day 2 and then harvested at day 4. Rates of cell proliferation were determined using Click-iT EdU Alexa Fluor 488 Cell Proliferation Assay Kit for flow cytometry (Invitrogen).

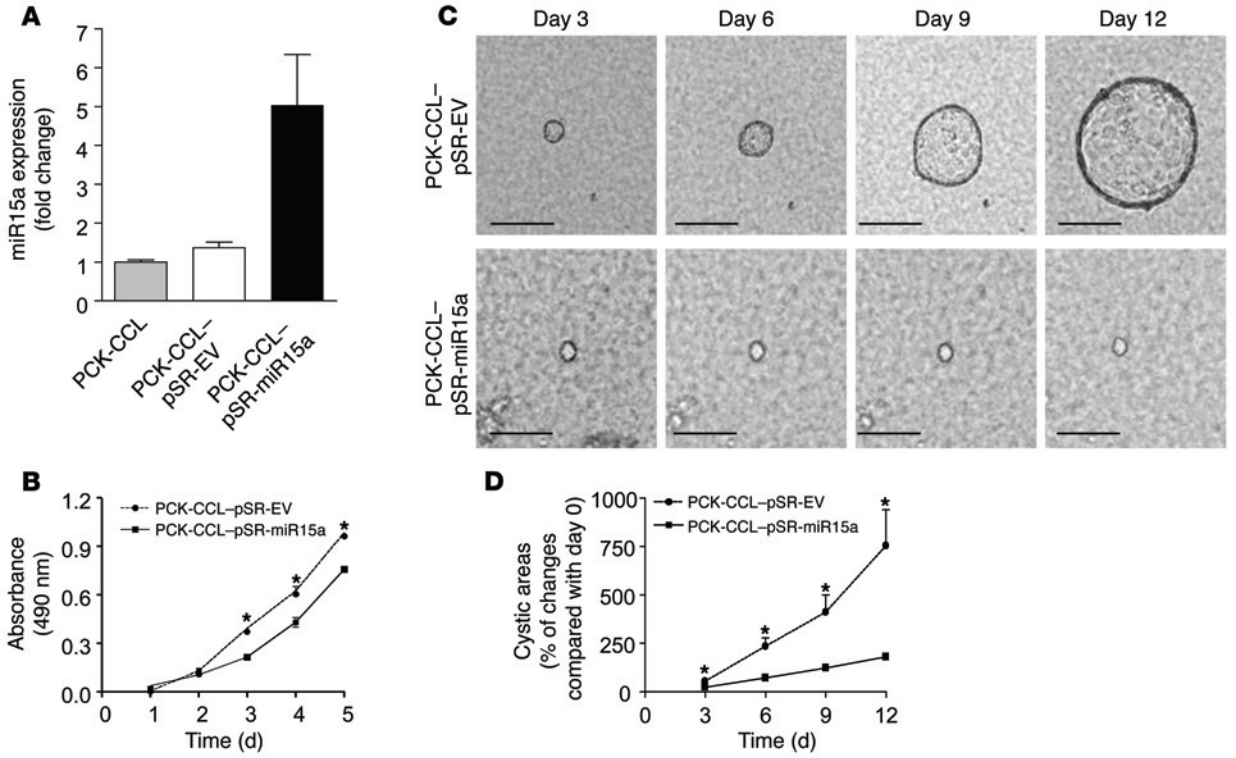

Figure 8
Effect of miR15a overexpression in cystic cholangiocytes on miR15a levels, cell proliferation, and cyst growth. (**A**) Quantitative PCR shows that in PCK-CCL stably transfected with the miR15a precursor (PCK-CCL–pSR-miR15a), levels of miR15a were increased compared with those in untransfected PCK-CCL or PCK-CCL transfected with EV (PCK-CCL–pSR-EV). (**B**) Cell proliferation was inhibited in PCK-CCL–pSR-miR15a compared with that in PCK-pSR-EV. Data are representative of 3 independent experiments. (**C**) Light microscopy analysis of PCK-CCL–pSR-EV and PCK-CCL–pSR-miR15a revealed the presence of cystic structures in 3D culture. Cysts formed by PCK-CCL–pSR-EV (top panels) continued to grow progressively over time while cystic structures formed by PCK-CCL–pSR-miR15a (bottom panels) did not expand. Scale bars: 250 μm. (**D**) Quantitative analysis of cystic areas demonstrates that rates of cyst growth in PCK-CCL–pSR-miR15a cultures (n = 13) were inhibited significantly compared with those in PCK-CCL–pSR-EV cultures (n = 25). *P < 0.05.

RNA isolation and RT-PCR. RNA was isolated from freshly isolated or cultured cholangiocytes with TRIzol Reagent (Invitrogen) and cDNA synthesized using the SuperScript III kit (Invitrogen). Primers corresponding to 5′ and 3′ regions of the Cdc25A (forward, AAGGCAAACCTGTTAAGTGTG; reverse, GGGTACACTTCAACATTCCAG), were designed and synthesized by Mayo Advanced Genomics Technology Center. PCR was performed for 35 cycles, each consisting of denaturation at 94°C for 1 minute, annealing at 55°C for 1 minute, and extension at 72°C for 1 minute. 18S rRNA was amplified to confirm an equal amount of total mRNA in samples and was used as normalized control. The intensity of the signals was quantified using a PhosphorImager (Molecular Dynamics Inc.). Sequencing was performed on all positive PCR products (Mayo Advanced Genomics Technology Center) to confirm the identity of amplified genes.

To measure miR15a levels, a quantitative PCR approach using a LightCycler (Roche) was employed. Expression of miR15a was assessed according to the TaqMan MicroRNA Assay protocol (Applied Biosystems). cDNA was synthesized from 2 μg of total RNA using miR15a-specific primers and the TaqMan MicroRNA Reverse Transcription Kit (both from Applied Biosystems). PCR for miR15a was performed for 45 cycles at 95°C for 15 seconds, and annealing and extension steps were performed at 59°C. The data were analyzed using the comparative Ct method. Data are given as fold changes of average signals in normal and cystic cholangiocytes.

Immunofluorescence microscopy. NRCs and PCK-CCL were grown on cover slips, fixed with methanol (5 minutes at –20°C), and incubated overnight at 4°C with primary antibodies against acetylated tubulin (Sigma-Aldrich) at a dilution of 1:100 or Cdc25A (Santa Cruz Biotechnology Inc.) at a dilution of 1:100. Alexa Fluor 488 and Alexa Fluor 594 (Invitrogen) were used as secondary antibodies (1:500 dilution), and nuclei were stained with DAPI.

Western and Northern blot analysis. Total protein was extracted with M-PER Mammalian Protein Extraction Reagent (Pierce; Thermo Scientific), separated by sodium dodecyl sulfate/polyacrylamide electrophoresis, and transferred overnight to a nitrocellulose membrane; Cdc25A was detected using primary Cdc25A antibody (1:500 dilution; Santa Cruz Biotechnology Inc.) and horseradish peroxidase–conjugated goat anti-mouse secondary antibody (1:1000 dilution; Sigma-Aldrich). β-actin served as a loading control. Protein bands were detected using an enhanced chemiluminescence detection system (Amersham; GE Healthcare).

For Northern blot, miRNAs were enriched from the total RNA (mirVana miRNA Isolation kit, Ambion; Applied Biosystems). miRNAs (1 μg) were separated on a 15% polyacrylamide gel and transferred to membrane. The probes for miRNAs and 5S RNA detections were synthesized using templates for miR15a (5′-TAGCAGCACATAATGGTTTGTGCCTGTCTC-3′, and 5S RNA (5′-GTTAGTACTTGGATGGGAGACCGCCCTGTCTC-3′). After incubation with 2.5×10^6 cpm per blot overnight at 42°C, membranes were washed and exposed to autoradiography films for 24–96 hours.

Flow cytometry. PCK-CCL transfected with miR15a was harvested, fixed with cold 70% EtOH, and suspended in propidium iodide (50 μg/ml);

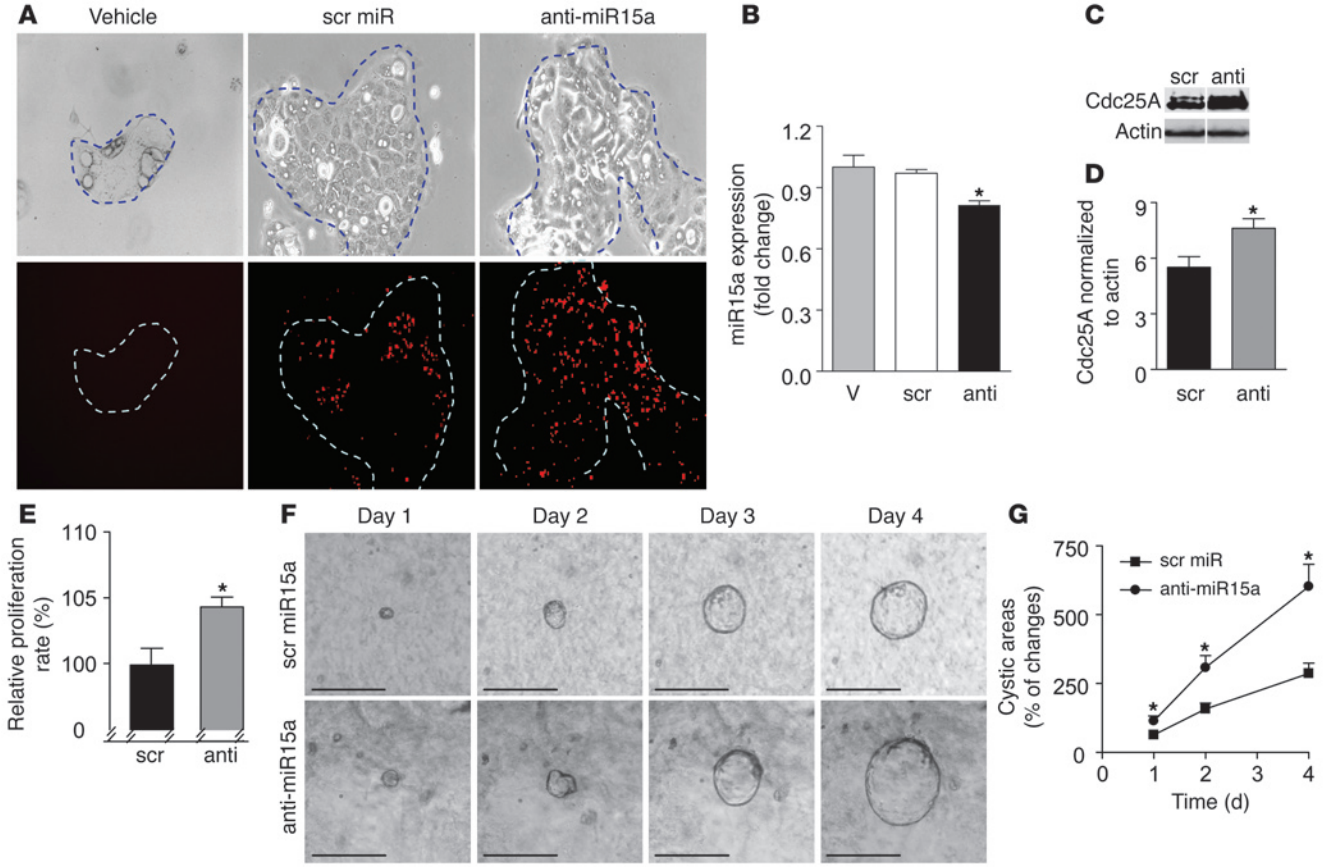

Figure 9
Effect of miR15a suppression in normal cholangiocytes on miR15a levels, Cdc25A expression, cell proliferation, and cyst growth. (**A**) Representative light (top panels) and fluorescent (bottom panels) images show that both scrambled miRNA and anti-miR15a were present in cultured cells in contrast with cholangiocytes treated with vehicle. Original magnification, ×20. (**B**) Quantitative PCR demonstrates that levels of miR15a in cholangiocytes treated with anti-miR15a (anti) were decreased compared with those in cholangiocytes treated with vehicle or scrambled miRNA. Data are representative of 3 independent experiments. (**C**) Representative Western blot and quantitative analysis based on densitometry measurements (**D**) of 5 independent experiments show that in anti-miR15a cholangiocytes, Cdc25A protein levels were increased by 38%. Thin white lines on the gel indicate that the lanes were run on the same gel but were noncontiguous. (**E**) Rates of cell proliferation were assessed in cholangiocytes treated with scrambled miRNA ($n = 5$) or anti-miR15a ($n = 6$) and expressed as a percentage of changes compared with rates of proliferation in nontreated cholangiocytes (considered to be equal to 100%). Cholangiocytes exposed to miR15a antisense display higher rates of proliferation than cholangiocytes exposed to scrambled miRNA. (**F**) Representative light microscopic images of cystic structures formed in 3D culture by normal cholangiocytes and quantitative assessment of changes in cystic areas over time (**G**) reveal that in the presence of anti-miR15a, cysts grow more rapidly compared with those in the presence of scrambled miRNA. Changes shown in **G** are in comparison with day 0. *$P < 0.05$. Scale bars: 250 μm.

RNase A (0.1 mg/ml) was added. After incubation at 37°C for 30–45 minutes, FACS analysis was performed at Mayo Advanced Genomics Technology Center.

Microarray analysis of endogenous miRNA expression. miRNA expression profiling of NRCs and PCK-CCL was performed using GenoExplorer Microarray Biochip Platform (GenoSensor Corp.) that contains 254 miRNA sequences selected from the public database. 10 μg of total RNA was isolated from normal and cystic cholangiocytes and then labeled and hybridized to a commercial microarray for analysis by the GenoSensor Corp. under optimized conditions. The average of 3 mean fluorescence signal intensities for each precursor miRNA probe was normalized to that for $tRNA^{met}$. Precursor miRNAs detected at 2-fold greater than background were considered to be expressed. Data were analyzed with GenePix 5.0 software, provided by GenoSensor Corp.

Prediction of miRNA targets. Three well-known miRNA target prediction programs were used to search for miR15a targets: TargetScan 4.1 (http://www.targetscan.org), miRBase Targets Version 5 (http://microrna.sanger.ac.uk/targets/v5/), and PicTar (http://pictar.bio.nyu.edu). Through all of these programs, Cdc25A was identified as a predicted target of miR15a (conserved in human, mouse, and rat).

Genomic DNA PCR. 0.1 μg of genomic DNA was amplified using miR15a precursor–specific primers: sense (5′-AAGGCAAACCTGTTAAGTGTG-3′) and antisense (5′-GCACATCCAGTGATGGGTTT-3′). Each amplification reaction consisted of 35 cycles at 94°C for 1 minute, 55°C for 1 minute, and 72°C for 1 minute. PCR product was sequenced by Mayo Advanced Genomics Technology Center.

In situ hybridization. Liver tissue sections were deparaffinized, washed in PBS and deproteinated with proteinase K (10 μg/ml at 37°C). Sections were washed once in 0.2% glycine in PBS and twice in PBS, then fixed for 10 minutes in 4% PFA. Prehybridization was performed in a humidified chamber (50% formamide, 5X SSC) using hybridization buffer (50% for-

mamide, 5X SSC, 0.1% Tween, 9.2 mM citric acid for adjustment to pH 6, 50 μg/ml heparin, and 500 μg/ml yeast RNA) for 2 hours. Slides were then hybridized overnight with 20 nM of FITC-labeled miR15a (CACAAACCATTATGTGCTGCTA) or scrambled miRNA (TTCACAATGCGTTATCGGATGT; Exiqon) in a humidified chamber at 51°C. Liver sections were rinsed in 2X SSC, washed 3 times for 30 minutes in 50% formamide and 2X SSC at hybridization temperature, and washed 5 times for 5 minutes in PBST at room temperature.

Establishment of transiently and stably transfected PCK-CCL. PCK-CCL (60%–70% confluent) was transfected using siPORT NeoFx Lipid-Based Reverse Transfection Reagent (AM-4511, Ambion; Applied Biosystems) or FuGENE Transfection Reagent (Roche), respectively. In brief, 5 μl of siPORT NeoFx was mixed with 100 μl of Opti-MEM (Invitrogen), incubated for 10 minutes at room temperature, and then incubated for an additional 10 minutes with 20 nM (final dilution) of miR15a precursor oligonucleotides. PCK-CCL (2.5×10^5 cells) were suspended in this solution and plated. Western blot analysis for Cdc25A was performed 12 hours after transfection. PCK-CCL transiently transfected with FITC-labeled miR15a was used for confocal microscopy.

For FuGENE transfection, 3 μl of FuGENE Transfection Reagent (Roche) was added to 97 μl of Opti-MEM and incubated for 5 minutes at room temperature. 20 nM (final dilution) of miR15a precursor oligonucleotides were added to the FuGENE/Opti-MEM mixture, incubated for an additional 15 minutes, and applied to PCK-CCL (60%–70% confluent). Flow cytometry (FACS) analysis was performed 12 hours after transfection.

To establish a stably transfected PCK-CCL, a p*Silencer* vector (Ambion; Applied Biosystems) was constructed by inserting an 83-bp genomic sequence of miR15a precursor (PCK-CCL–pSR-miR15a). We used the following oligonucleotides for the top strand and bottom strand, respectively: 5′-GATCCGCCCTTGGAGTAAAGTAGCAGCACATAATGGTTTGTGGA-TGTTGAAAAGGTGCAGGCCATACTGTGCTGCCAAAATACAAGGAGGAAA-3′ and 5′-AGCTTTTCCTCCTTGTATTTTGAGGCAGCACAGTATG-GCCTGCACCTTTTCAACATCCACAAACCATTAGTGCTGCTACTTTACTCCAAGGGCG-3′. The oligos were annealed and subsequently ligated with T4 DNA ligase into the p*Silencer* 4.1–CMV (Ambion; Applied Biosystems) expressing the puromycin cassette. PCK-CCL transfected with this plasmid construct and stably transfected cells were selected using puromycin (1 μg/ml).

Luciferase reporter constructs and luciferase assay. A 436-bp fragment of the 3′-UTR region of rat Cdc25A mRNA that contains the miR15a target site was amplified by RT-PCR using specific primers sense 5′-TGAGTACTAGTCCTTCCCTGTCAGGACTG-3′ and anti-sense 5′-CAGCTAAGCTTGCGCTGCCCACACTTAAC-3′ and cloned into pMIR-REPORT luciferase vector (Ambion; Applied Biosystems). The mutant Cdc25A mRNA 3′-UTR region (TGCTGCTG to TGCACCAG) was also constructed. PCK-CCL was transfected with each construct miR15a precursor oligonucleotide or scrambled miRNA, followed by assessment of luciferase activity at 48 hours after transfection. Luciferase activity was normalized to TK Renilla construct as previously reported (40).

3D culture and cyst measurement. The cystic and normal cholangiocytes were grown in 3D culture as previously described (12). To study the effect of miR15a overexpression we used stable-transfected PCK-CCL. Development of cystic structures was assessed by light microscopy at day 3 after seeding, and each cyst was followed up at days 6, 9, and 12. To study the effect of miR15a suppression on cyst growth, NRCs were seeded in 3D culture and treated with 50 nM of either anti-miR15a (Ambion; Applied Biosystems) or scrambled miRNA at days 0 and 2. Growth of cystic structures was assessed by light microscopy for 5 consecutive days. Using ImageJ software (http://rsbweb.nih.gov/ij/), we determined the cross-sectional area of normal and PCK cysts; data were expressed as a percentage of changes in cystic area compared with day 0 (i.e., day when cells were entered in 3D culture).

Statistics. All values were expressed as mean ± SEM. Statistical analysis was performed by 2-tailed Student's *t* test, and results were considered statistically significant at $P < 0.05$.

Acknowledgments

This work was supported by grant DK24031 from the NIH (to N.F. LaRusso), grant 02TRN07a from the PKD Foundation (to T.V. Masyuk), grant KRF-2005-214-C00114 from the Korea Research Foundation (to S.-O. Lee), a grant from the Spanish Ramón Areces Foundation, Spain (to J.M. Banales), and by the Mayo Foundation.

Received for publication January 3, 2008, and accepted in revised form September 17, 2008.

Address correspondence to: Nicholas F. LaRusso, Miles and Shirley Fiterman Center for Digestive Diseases, Mayo Clinic College of Medicine, 200 First Street SW, Rochester, Minnesota 55905, USA. Phone: (507) 284-1006; Fax: (507) 284-0762; E-mail: larusso.nicholas@mayo.edu.

Seung-Ok Lee, Tatyana Masyuk, and Patrick Splinter contributed equally to this work.

1. Masyuk, T., and LaRusso, N. 2006. Polycystic liver disease: new insights into disease pathogenesis. *Hepatology.* **43**:906–908.
2. Everson, G.T., Taylor, M.R., and Doctor, R.B. 2004. Polycystic disease of the liver. *Hepatology.* **40**:774–782.
3. Drenth, J.P., Martina, J.A., Te Morsche, R.H., Jansen, J.B., and Bonifacino, J.S. 2004. Molecular characterization of hepatocystin, the protein that is defective in autosomal dominant polycystic liver disease. *Gastroenterology.* **126**:1819–1827.
4. Chang, M.Y., and Ong, A.C. 2008. Autosomal dominant polycystic kidney disease: recent advances in pathogenesis and treatment. *Nephron Physiol.* **108**:p1–p7.
5. Onuchic, L.F., et al. 2002. PKHD1, the polycystic kidney and hepatic disease 1 gene, encodes a novel large protein containing multiple immunoglobulin-like plexin-transcription-factor domains and parallel beta-helix 1 repeats. *Am. J. Hum. Genet.* **70**:1305–1317.
6. Ward, C.J., et al. 2002. The gene mutated in autosomal recessive polycystic kidney disease encodes a large, receptor-like protein. *Nat. Genet.* **30**:259–269.
7. Shneider, B.L., and Magid, M.S. 2005. Liver disease in autosomal recessive polycystic kidney disease. *Pediatr. Transplant.* **9**:634–639.
8. Katsuyama, M., Masuyama, T., Komura, I., Hibino, T., and Takahashi, H. 2000. Characterization of a novel polycystic kidney rat model with accompanying polycystic liver. *Exp. Anim.* **49**:51–55.
9. Masyuk, T.V., et al. 2004. Biliary dysgenesis in the PCK rat, an orthologous model of autosomal recessive polycystic kidney disease. *Am. J. Pathol.* **165**:1719–1730.
10. Masyuk, T.V., Masyuk, A.I., Torres, V.E., Harris, P.C., and Larusso, N.F. 2007. Octreotide inhibits hepatic cystogenesis in a rodent model of polycystic liver disease by reducing cholangiocyte adenosine 3′,5′-cyclic monophosphate. *Gastroenterology.* **132**:1104–1116.
11. Lager, D.J., Qian, Q., Bengal, R.J., Ishibashi, M., and Torres, V.E. 2001. The pck rat: a new model that resembles human autosomal dominant polycystic kidney and liver disease. *Kidney Int.* **59**:126–136.
12. Muff, M.A., et al. 2006. Development and characterization of a cholangiocyte cell line from the PCK rat, an animal model of autosomal recessive polycystic kidney disease. *Lab. Invest.* **86**:940–950.
13. Karlsson-Rosenthal, C., and Millar, J.B. 2006. Cdc25: mechanisms of checkpoint inhibition and recovery. *Trends Cell Biol.* **16**:285–292.
14. Sadhu, K., Reed, S.I., Richardson, H., and Russell, P. 1990. Human homolog of fission yeast cdc25 mitotic inducer is predominantly expressed in G2. *Proc. Natl. Acad. Sci. U. S. A.* **87**:5139–5143.
15. Galaktionov, K., and Beach, D. 1991. Specific activation of cdc25 tyrosine phosphatases by B-type cyclins: evidence for multiple roles of mitotic cyclins. *Cell.* **67**:1181–1194.
16. Boutros, R., Dozier, C., and Ducommun, B. 2006. The when and wheres of CDC25 phosphatases. *Curr. Opin. Cell Biol.* **18**:185–191.
17. Kristjansdottir, K., and Rudolph, J. 2004. Cdc25 phosphatases and cancer. *Chem. Biol.* **11**:1043–1051.
18. Prevost, G.P., et al. 2003. Inhibitors of the CDC25

phosphatases. *Prog. Cell Cycle Res.* **5**:225–234.
19. Miska, E.A. 2005. How microRNAs control cell division, differentiation and death. *Curr. Opin. Genet. Dev.* **15**:563–568.
20. Carthew, R.W. 2006. Gene regulation by microRNAs. *Curr. Opin. Genet. Dev.* **16**:203–208.
21. Chan, J.A., Krichevsky, A.M., and Kosik, K.S. 2005. MicroRNA-21 is an antiapoptotic factor in human glioblastoma cells. *Cancer Res.* **65**:6029–6033.
22. Cimmino, A., et al. 2005. miR-15 and miR-16 induce apoptosis by targeting BCL2. *Proc. Natl. Acad. Sci. U. S. A.* **102**:13944–13949.
23. Hwang, H.W., and Mendell, J.T. 2006. MicroRNAs in cell proliferation, cell death, and tumorigenesis. *Br. J. Cancer.* **94**:776–780.
24. Calin, G.A., and Croce, C.M. 2006. MicroRNA-cancer connection: the beginning of a new tale. *Cancer Res.* **66**:7390–7394.
25. Lu, J., et al. 2005. MicroRNA expression profiles classify human cancers. *Nature.* **435**:834–838.
26. Wienholds, E., et al. 2005. MicroRNA expression in zebrafish embryonic development. *Science.* **309**:310–311.
27. Nelson, P.T., et al. 2006. RAKE and LNA-ISH reveal microRNA expression and localization in archival human brain. *RNA.* **12**:187–191.
28. Johnson, C.D., et al. 2007. The let-7 microRNA represses cell proliferation pathways in human cells. *Cancer Res.* **67**:7713–7722.
29. Tian, Z., Greene, A.S., Pietrusz, J.L., Matus, I.R., and Liang, M. 2008. MicroRNA-target pairs in the rat kidney identified by microRNA microarray, proteomic, and bioinformatic analysis. *Genome Res.* **18**:404–411.
30. Bak, M., et al. 2008. MicroRNA expression in the adult mouse central nervous system. *RNA.* **14**:432–444.
31. Porkka, K.P., et al. 2007. MicroRNA expression profiling in prostate cancer. *Cancer Res.* **67**:6130–6135.
32. Yanaihara, N., et al. 2006. Unique microRNA molecular profiles in lung cancer diagnosis and prognosis. *Cancer Cell.* **9**:189–198.
33. Chauveau, D., Fakhouri, F., and Grunfeld, J.P. 2000. Liver involvement in autosomal-dominant polycystic kidney disease: therapeutic dilemma. *J. Am. Soc. Nephrol.* **11**:1767–1775.
34. O'Donnell, K.A., Wentzel, E.A., Zeller, K.I., Dang, C.V., and Mendell, J.T. 2005. c-Myc-regulated microRNAs modulate E2F1 expression. *Nature.* **435**:839–843.
35. Lee, Y., et al. 2004. MicroRNA genes are transcribed by RNA polymerase II. *EMBO J.* **23**:4051–4060.
36. Lund, E., Guttinger, S., Calado, A., Dahlberg, J.E., and Kutay, U. 2004. Nuclear export of microRNA precursors. *Science.* **303**:95–98.
37. Thomson, J.M., et al. 2006. Extensive post-transcriptional regulation of microRNAs and its implications for cancer. *Genes Dev.* **20**:2202–2207.
38. Bukanov, N.O., et al. 2006. Long-lasting arrest of murine polycystic kidney disease with CDK inhibitor roscovitine. *Nature.* **444**:949–952.
39. Vroman, B., and LaRusso, N.F. 1996. Development and characterization of polarized primary cultures of rat intrahepatic bile duct epithelial cells. *Lab. Invest.* **74**:303–313.
40. Chen, X.M., et al. 2005. Multiple TLRs are expressed in human cholangiocytes and mediate host epithelial defense responses to Cryptosporidium parvum via activation of NF-kappaB. *J. Immunol.* **175**:7447–7456.